Can Cassini Magnetic Field Measurements Be Used To Find The Rotation Period of Saturn's Interior?

Share Your Story

The Harvard community has made this article openly available.
Please share how this access benefits you. Submit a story .

Accessibility

Can Cassini magnetic field measurements be used to find the rotation period of Saturn's interior?

M. Glenn Sterenborg[1] and Jeremy Bloxham[1]

[1] We investigate the determination of the rotation period of Saturn's interior using magnetic field measurements from Cassini. First, we vary the rotation period and search for the period that yields the smallest rms misfit of a magnetic field model to the data. Second, we search for the period that yields the most power in the non-axisymmetric components of a magnetic field model. Neither method enables us to determine the rotation period. However, we are able to place a bound on the magnitude of the non-axisymmetric component of Saturn's magnetic field finding it to be no greater than 4–5% of the axisymmetric component. **Citation:** Sterenborg, M. G., and J. Bloxham (2010), Can Cassini magnetic field measurements be used to find the rotation period of Saturn's interior?, *Geophys. Res. Lett.*, *37*, L11201, doi:10.1029/2010GL043250.

1. Introduction

[2] Accurate knowledge of the rotation period of a planet's interior is a critical prerequisite to understanding many aspects of a planet's dynamics. In the case of Saturn, the rotation period is poorly constrained, and has been hotly debated for many years; we summarize various determinations of the rotation period in Table 1 from which the large uncertainty in the rotation period is apparent.

[3] In this article, following the results of [*Giampieri et al.*, 2006], we investigate whether Saturn's internal rotation period can be determined from Cassini magnetic field (MAG) data. In section 2 we discuss our approach, how we model the magnetic field and how we remap longitudes for a choice of rotation period. We test our approach in section 3 and determine the signature of rotation in magnetic field observations. Finally, in section 4 we apply our methods to Cassini data.

2. Approach

[4] We use a straightforward approach. We start with the IAU rotation period of Saturn as a reference point in a grid search for a planetary rotation period that gives a minimum rms misfit of a magnetic field model with respect to MAG data. For every choice of rotation period we remap the longitudes, from the MAG data, which are based on the IAU period, to pseudolongitudes. We use these remapped data to construct a magnetic field model and compute the consequent rms misfit to the data and the ratio of non-axisymmetric to axisymmetric power in the solution. Assuming a non-

axisymmetric component is present in Saturn's magnetic field, an incorrect choice of rotation period will cause us to assign longitudes to the magnetic field measurements that change for data which, in reality, are acquired at a fixed longitude, but at different times. This will cause the non-axisymmetric component to be smeared out and will render it harder to resolve. For the choice of rotation period that equals Saturn's 'true' rotation period we expect to find a maximum in the power ratio, and concomitantly a minimum in the rms misfit.

[5] The dataset we use ranges from January 2004 to May 2008 with the bulk of the data between −30° and 20° latitude. Although data after this period are available at NASA's Planetary Data System, our analysis has revealed that the trajectory information for this period contains errors, as confirmed by J. Wolf (personal communication, 2009), and as such is discarded. Unfortunately during this time Cassini approached Saturn closely at high latitudes which would have been helpful in resolving small wavelength features in Saturn's magnetic field.

2.1. Magnetic Field Model

[6] We construct models of Saturn's magnetic field using the canonical spherical harmonic basis functions. Using a weighted linear least-squares estimation we estimate the internal and external field using only data within 3.9 R_S, i.e. within Enceladus' orbit, implicitly assuming that this region is current-free. We weight the data by the number of measurements per 1 minute averaged data point. Although the source field is infinite band, our estimate of it necessarily has to be band limited since the dataset is finite. In producing models of Saturn's magnetic field we generally regularize the solution using a smoothing norm and truncate at sufficiently high degree to ensure that our solutions are numerically converged, [*Wahler and Gubbins*, 1981; *Gubbins and Bloxham*, 1985]. However in this study, we truncate at degree 4 and do not regularize because as we expect the non-axisymmetric signature to be very small: any damping might yield models that are too smooth to find a minimum in the rms misfit to the data.

2.2. Remapping Longitudes

[7] To carry out the grid search for the rotation period that yields a magnetic model with the smallest rms misfit to the data we must remap the longitudes from the reference body-fixed coordinate frame rotating with a reference period to another body-fixed frame rotating with a different period.

[8] Specifying that two coordinate frames start from the same position at time t_{ref}, we can express the new longitude (ϕ_2) as a function of the old longitude (ϕ_1)

$$\phi_2 = \phi_1 + \Delta\phi \qquad (1)$$

---

[1]Department of Earth and Planetary Sciences, Harvard University, Cambridge, Massachusetts, USA.

Table 1. Estimates of Saturn's Rotation Periods[a]

Period (h min s)	Method
10 14 – 10 42	Cloud tracking[a]
10 39 24 ± 7	SKR modulation[b]
10 45 45 ± 36	SKR modulation[c]
10 47 6 ± 40	Magnetic field measurement[d]
10 32 35 ± 13	Gravity and zonal wind[e]
10 34 13 ± 20	Potential vorticity[f]

[a]*Sanchez-Lavega* [1982].
[b]*Desch and Kaiser* [1981].
[c]*Gurnett et al.* [2005].
[d]*Giampieri et al.* [2006].
[e]*Anderson and Schubert* [2007].
[f]*Read et al.* [2009].

where $\Delta\phi$ can be written as

$$\Delta\phi = (\omega_1 - \omega_2) \cdot (t - t_{ref})$$
$$= 2\pi\left(\frac{1}{T_1} - \frac{1}{T_2}\right) \cdot (t - t_{ref})$$
$$= 2\pi\left(\frac{1}{T_1} - \frac{1}{T_1 - \Delta T}\right) \cdot (t - t_{ref}) \qquad (2)$$
$$= -2\pi\left(\frac{\Delta T}{T_1(T_1 - \Delta T)}\right) \cdot (t - t_{ref})$$

where $\omega_{1,2}$ is the old and new rotation rate respectively. $T_{1,2}$ is the old and new rotation period respectively with the convention that $T_2 = T_1 - \Delta T$. If $T_2 < T_1$ then $\Delta T > 0$ which yields $\Delta\phi < 0$ and the opposite for $T_2 > T_1$. In remapping longitudes we take the first time record as t_{ref}.

3. Test Cases

[9] Before applying our method to the Cassini MAG data we examine a number of test cases where we *a priori* specify the magnetic field to be sampled. We are interested how our method performs for noisy data, to what extent it can resolve the minimum in the rms misfit if the strength of the input (non-axisymmetric) magnetic field is varied, or if we vary the choice of degree and order of the non-axi-

symmetric field. In the next section we will see that the misfit does not vary smoothly away from the minimum. Besides the magnetic field we also *a priori* specify (for our test data set) the planet's true rotation period, as well as the rotation period we take as a reference in the grid search. We further specify the level of noise in the synthetic data, the number of sampling points, the trajectories along which these are taken and the times at which they are taken.

3.1. A Tilted Dipole

[10] We start with a field that has a dipole component similar in strength to that typically found for Saturn, $g_1^0 = 2 \times 10^4$ nT, and add a strong non-axisymmetric component, $g_1^1 = 2 \times 10^3$ nT. We use Cassini trajectories (<3.9 R_S) and sampling frequency to sample the field in the same way as the actual data. We specify a true rotation period of IAU (10 hr 39 m 42 s) + 350 seconds (the offset is arbitrarily chosen). We use this rotation period to sample the field in time; however, the data we use in constructing the magnetic field models have longitudes based on the reference rotation period. We choose the IAU period as the reference and search up to 10 minutes either side of it with a timestep of 1.2 seconds. In other words, we construct ~1000 magnetic field models. The results are shown in Figures 1 and 2.

[11] It is clear where the true rotation period is, both from the rms misfit plot and the power ratio plot. We note that the minimum is very sharply defined, indicating that a small time step is required to detect the minimum. The rms misfit at the minimum is at ~10 nT, the specified noise level, which is as expected. Had we used perfect data, i.e. without simulated noise, the misfit would have been zero. Away from the minimum, the rms misfit varies around an average value. This 'plateau' corresponds to rotation periods for which the remapped longitudes have spread out around the axis, and so the non-axisymmetric field effectively becomes a source of noise. As such, the plateau level v is determined by the magnitude of the non-axisymmetric component of the magnetic field at the spacecraft's average radial distance from the planet, r_{avg}, which, for this case, yields $v \propto g_1^1(R_S/r_{avg})^3$, with R_S the planetary radius. For more complicated non-axisymmetry in the magnetic field a similar relationship can
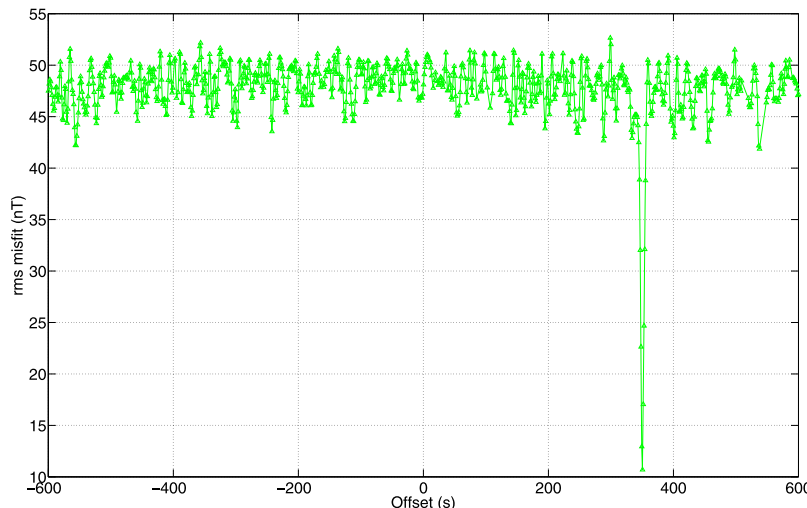

Figure 1. RMS misfit vs offset for a tilted dipole $g_1^0 = 2 \times 10^4$ nT, $g_1^1 = 2 \times 10^3$ nT with added gaussian noise of 10 nT standard deviation. True period specified at IAU + 350 seconds.

Figure 2. Ratio of non-axisymmetric and axisymmetric power per degree vs offset for a tilted dipole $g_1^0 = 2 \times 10^4$ nT, $g_1^1 = 2 \times 10^3$ nT with added gaussian noise of 10 nT standard deviation. True period specified at IAU + 350 seconds.
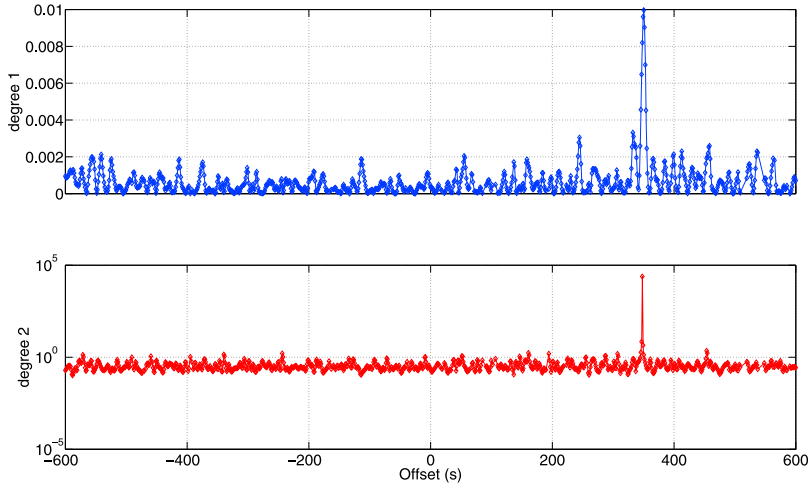
be found. One might intuitively expect the rms misfit to smoothly vary away from the minimum to a maximum value. We investigate this further in the next section, and also address what governs the slope away from the minimum with a simpler test case in the next section.

[12] Figure 2 shows that we not only resolve the true period in degree 1, where we specified the non-axisymmetric power to be, but also in degree 2, indicating that given the spatial data coverage the spherical harmonics are not completely separated in this case.

3.2. Narrow Minimum and the Noisy Plateau

[13] Why do we observe a sharp minimum and a noisy plateau? The former has implications on the timestep we use in the grid search. If we use too large a step a sharp minimum may go unnoticed. The latter may obscure a minimum altogether. To investigate the slope away from the minimum we vary the degree l and order m of the non-axisymmetric field g_l^m as we expect the slope to steepen with decreasing wavelength of the non-axisymmetry present in the magnetic field. Varying the rotation period will more readily reorganize, through the longitude remapping, a small wavelength non-axisymmetric field than a long wavelength one. We find that for increasing l this is a minor effect, whereas for increasing m the effect is much more prominent. This is likely due to the trajectories used to sample the field which are largely equatorial and so more sensitive to azimuthal structure in the field as opposed to meridional structure. An equatorial dipole will, therefore, result in the broadest possible minimum. We also note that the slope does not vary with strength of the non-axisymmetry. Higher degree or order non-axisymmetric power will increase the noise level of the plateau while noise in the data will make the minimum less deep. Either of these aspects, or a combination of them, can result in the minimum being hidden.

[14] To investigate the noise in the plateau in Figure 1 we adopt a further test. We use an equatorial dipole, $g_1^1 = 2 \times 10^4$ nT, as an input field, set the true rotation period at 10 hours and sample the field at two distinct epochs. Unlike previous tests where we sampled the field along Cassini trajectories, we now sample the field globally at 250 locations for each epoch, resulting in a dataset with 500 simulated data

half at the first epoch and half at the second. The resulting rms misfit varies nearly periodically with rotation period with a ΔT_{bm} seconds step interval between minima. We find that the ratio of the difference between the two epochs, Δt, and the choice of rotation period yields an integer change in the number of planetary rotations for a ΔT_{bm} seconds step in rotation period. It changes slightly for additional minima because adding an integer number of ΔT_{bm} does not exactly yield an integer change of planetary rotations. Thus for an integer change in the number of planetary rotations ΔT_{bm} will drift slightly.

[15] We repeated this test with sampling at four epochs and noted two important consequences. First, we do not achieve coherency with a decrease in Δt. Δt is now small enough that an addition of it to a choice of rotation period, within the grid search range, will not result in an integer change of the number of planetary rotations between consecutive epochs. However, a small measure of coherency is achieved, which is the cause of the fluctuations, i.e. noise, in the result. Second, for four epochs the slope away from the
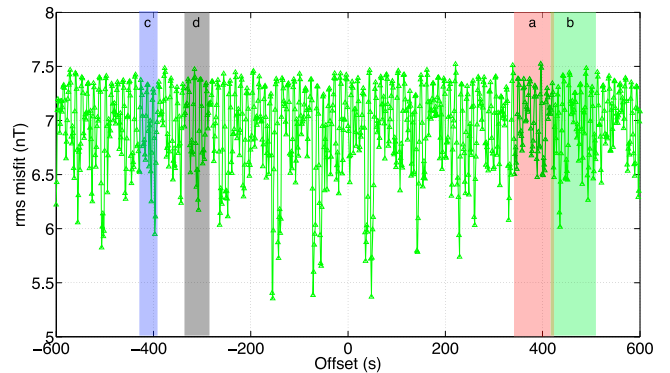

Figure 3. RMS misfit vs offset for Cassini data, January 2004 to May 2008, within 3.9 R_S. Magnetic field models were truncated at degree 4 for the internal field and degree 1 for the external field. Transparent bars indicate rotation periods, including uncertainties, as determined by others. (a) *Gurnett et al.* [2005], (b) *Giampieri et al.* [2006], (c) *Anderson and Schubert* [2007], (d) *Read et al.* [2009].
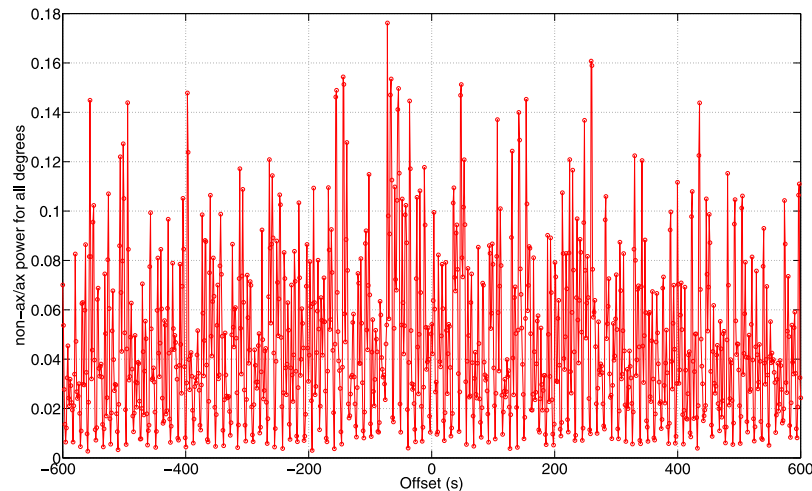
Figure 4. Ratio of non-axisymmetric and axisymmetric power vs offset for Cassini data, January 2004 to May 2008, within 3.9 R_S. Magnetic field models were truncated at degree 4 for the internal field and degree 1 for the external field.

minimum is much steeper indicating there may be a balance between using as many data as possible, to obtain a good field model, and subsampling the dataset, to more easily find the minimum in the rms misfit.

4. Cassini Results

[16] To apply this method to the actual Cassini MAG data we select data from January 2004 to May 2008 within 3.9 R_S, giving ~9400 data. Each datum is a one minute average. We estimate the internal and external fields, truncating our model at degree 4 for the internal field and degree 1 for the external field (4;1). Having experimented with the truncation of the external field model we found truncating at degree 1 to be sufficient. Extra harmonics do not significantly affect the misfit to the data. We have also run (3;1) models with similar results. We assume the IAU rotation period as the reference period in the grid search which ranges from −600 to 600 seconds with a 1.2 second time step. Figure 3 shows the rms misfit with offset and reveals no clear global minimum but does show several local minima and shows a great deal of fluctuation, over a wide range of time scales. The plateau rms misfit is between 7 and 7.5 nT. As expected, the fluctuations are considerably more complex than in our tests of the previous section, which is due to using many more epochs, i.e. sampling times, as well as orbit geometry effects. We show the ratio of non-axisymmetric and axisymmetric power in Figure 4, which is similarly more complex. The ratio fluctuates strongly with offset from the reference period and we discern no clearly unique maximum. We do see some peaks when we look at this ratio per spherical harmonic degree (not shown here) but they mostly consist of single points and we consider them anomalies that do not carry any particular physical meaning.

[17] We have also tried this method with subsampling the dataset, using every 100th datum, thereby increasing the intervals between consecutive field measurements. This revealed more structure in the result and hinted at a global minimum between −55 and −75 seconds, but only slightly more prominent than the noise, within 0.25 nT of other nearby minima.

[18] We have noticed that when we run a damped (3;1) model data ($<3.9R_S$) using the IAU period, we find almost the same rms misfit,~7.5 nT as when we run a (3;1) forced axisymmetric model, with only $O(10^{-1})$ nT difference. A (4;1) damped model yields a similar difference in rms misfit. Revisiting Figure 3 we observe a plateau misfit of ~7.5 nT. This may indicate that the non-axisymmetric power is in degrees/orders beyond 3 or 4 where our models cannot resolve it but instead reveal it in the form of an increased misfit.

5. Conclusions

[19] We have shown that the rotation period of Saturn's interior cannot be determined from the Cassini data that are currently available. The reason for this is that any non-axisymmetric ingredients in Saturn's internal field are inadequately sampled by Cassini because they are too small, too small compared to either the axisymmetric field or to the noise in the observations, or some combination. In a related effort, *Burton et al.* [2009] reported finding an unambiguous rotation period. How to reconcile this given our findings is, at present, unclear.

[20] How small must the non-axisymmetric ingredients be? Assuming we have adequately accounted for external fields, and that axisymmetric and non-axisymmetric field ingredients are well separated, then the level of the misfit plateau may serve as a proxy for the power in the non-axisymmetric field. Taking the mean value of the ratio between non-axisymmetric to axisymmetric power as seen in Figure 4, yields ~4.5% of non-axisymmetric power. We note that direct determination of this ratio, that is by fitting a field model to data, requires accurate knowledge of the rotation period. If the rotation period is not known accurately, as is the case for Saturn, then direct determination will underestimate the ratio, in other words will result in field models that are more axisymmetric than the actual field.

References

Anderson, J., and G. Schubert (2007), Saturn's gravitational field, internal rotation, and interior structure, *Science*, *317*, 1384–1387.

Burton, M., et al. (2009), Saturn's rotation rate as determined from its non-axisymmetric magnetic field, *Eos Trans. AGU*, *90*(52), Fall Meet. Suppl., Abstract P53C-03.

Desch, M., and M. Kaiser (1981), Voyager measurement of the rotation period of Saturn's magnetic field, *Geophys. Res. Lett.*, *8*, 253–256.

Giampieri, G., et al. (2006), A regular period for Saturn's magnetic field that may track its internal rotation, *Nature*, *441*, 62–64.

Gubbins, D., and J. Bloxham (1985), Geomagnetic field analysis: III. Magnetic fields on the core - mantle boundary, *Geophys. J. R. Astron. Soc.*, *80*, 695–713.

Gurnett, D., et al. (2005), Radio and plasma wave observations at Saturn from Cassini's approach and first orbit, *Science*, *307*, 1255–1259.

Read, P., T. Dowling, and G. Schubert (2009), Saturn's rotation period from its atmospheric planetary-wave configuration, *Nature*, *460*, 608–610.

Sanchez-Lavega, A. (1982), Motions in Saturn's atmosphere: Observations before voyager encounters, *Icarus*, *49*(1), 1–16.

Wahler, K., and D. Gubbins (1981), Spherical harmonic analysis of the geomagnetic field: An example of a linear inverse problem, *Geophys. J. R. Astron. Soc.*, *65*, 645–693.

J. Bloxham and M. G. Sterenborg, Department of Earth and Planetary Sciences, Harvard University, Cambridge, MA 02138, USA. (mgsteren@fas.harvard.edu)